

Toward a microscopic description of flow near the jamming threshold

E. LERNER¹, G. DÜRING¹ and M. WYART¹

¹ *New York University, Center of Soft Matter Research - 4 Washington Place, New York, NY 10003, USA*

PACS 63.50.-x – Vibrational states in disordered solids
PACS 83.80.Hj – Rheology of suspensions
PACS 45.70.-n – Classical mechanics of granular systems

Abstract –We study the relationship between microscopic structure and viscosity in non-Brownian suspensions. We argue that the formation and opening of contacts between particles in flow effectively leads to a negative selection of the contacts carrying weak forces. We show that an analytically tractable model capturing this negative selection correctly reproduces scaling properties of flows near the jamming transition. In particular, we predict that (i) the viscosity η diverges with the coordination number z as $\eta \sim (z_c - z)^{-(3+\theta)/(1+\theta)}$, (ii) the operator which governs flow displays a low-frequency mode that controls the divergence of viscosity, at a frequency $\omega_{\min} \sim (z_c - z)^{(3+\theta)/(2+2\theta)}$, and (iii) the distribution of forces displays a scale f^* that vanishes near jamming as $f^*/\langle f \rangle \sim (z_c - z)^{1/(1+\theta)}$ where θ characterizes the distribution of contact forces $P(f) \sim f^\theta$ at jamming, and where z_c is the Maxwell threshold for rigidity.

Suspensions are heterogeneous fluids containing solid particles, whose viscosity was computed early on by Einstein [1] and Batchelor [2] in the dilute regime. As the packing fraction ϕ is increased however, steric hindrance becomes dominant and particles move under stress in an increasingly coordinated way [3–6]. For non-Brownian particles, the viscosity η eventually diverges as the suspension jams into an amorphous solid at some packing fraction ϕ_c . Recently, progress has been made in characterizing the rheological properties in this limit. It has been shown that non-Brownian suspensions [7–9], as well as aerial granular flows [10, 11], are characterized by two constitutive relations that relate the packing fraction ϕ and the macroscopic friction μ to the ratio of the local shear rate to the pressure. Both constitutive relations display singularities as jamming is approached, in particular it is observed that $\eta \sim (\phi_c - \phi)^{-a}$ where $a \approx 2$ [7]. This phenomenological description is valid beyond a length scale that grows near jamming, and below which non-local effects play a role [3, 8, 12]. There is currently no accepted microscopic description for this growing length scale, nor for the observed constitutive relations.

Olsson and Teitel [4, 13] and others [14, 15] have popularized a simplified model of non-Brownian suspensions where hydrodynamical interactions are neglected. We refer to the hard-particle limit of this model as the Affine

Solvent Model (ASM). The ASM constitutive relations are very similar to those found in real suspensions [16], supporting that it captures the essential physics near jamming. In this model it was observed that [16]: (i) there exists a scaling relation between the viscosity η and the coordination z : $\eta \sim (z_c - z)^{-2.85}$, where $z_c = 2D$ [17] and D is the spatial dimension. (ii) The dynamics is governed by one operator only. The material can thus be characterized by the spectrum of this operator, which contains more information than the constitutive relations. In flow, the spectrum displays bi-scaling near jamming, with a single mode being responsible for the fast divergence of the viscosity. In this Letter we explain these observations, make a new scaling prediction on the distribution of contact forces that we confirm empirically, and define and measure two new exponents characterizing contact forces both in flow and at jamming.

ASM is fully defined by the following three assumptions: (i) hydrodynamic interactions are neglected: the viscous drag on a particle is proportional to the difference $\vec{V}_{n.a.}$ between the particle velocity and the imposed velocity of the underlying fluid: $\vec{F} = -\xi_0 \vec{V}_{n.a.}$ where ξ_0 is a drag coefficient. The flow of the fluid phase is undisturbed by the particles and is chosen to be an affine simple shear of strain rate $\dot{\gamma}$. (ii) The dynamics is over-damped. (iii) Particles are hard, i.e. cannot overlap, and frictionless.

As is also the case for non-Brownian suspensions of hard particles [7, 9], within ASM rheological properties depend on only one dimensionless parameter, the normalized pressure $p \equiv p_p d^{D-2} / \dot{\gamma} \xi_0$ [16]. Here p_p is the particle pressure and d is the particle size. Near jamming the particle shear stress σ_p and pressure p_p are proportional $\mu \equiv \sigma_p / p_p \rightarrow \mu^* > 0$ [13, 18, 19], implying that the viscosity η and the renormalized pressure p are proportional too: $\eta \equiv \sigma_p / \dot{\gamma} \rightarrow (\xi_0 \mu^* / d^{D-2}) \times p$. These quantities depend only on the geometry of the network formed by particles in contact and can be expressed in a compact form [16]:

$$\eta = -\frac{\langle \gamma | f \rangle}{\dot{\gamma} \Omega D} = \frac{\xi_0}{\Omega} \langle \gamma | \mathcal{N}^{-1} | \gamma \rangle, \quad (1)$$

$$p_p = \frac{\langle r | f \rangle}{\Omega D} = -\frac{\dot{\gamma} \xi_0}{\Omega D} \langle r | \mathcal{N}^{-1} | \gamma \rangle, \quad (2)$$

where Ω is the volume of the system. $|r\rangle$ is the vector of dimension N_c – the total number of contacts made between the N particles – of the distances r_α between particles in contact. $|\gamma\rangle$ is a vector, also of dimension N_c , whose components are the variations of the contact lengths under an affine simple shear in the (x, y) plane: $\gamma_\alpha \equiv \partial r_\alpha / \partial \gamma \equiv (\vec{r}_\alpha \cdot \vec{e}_x)(\vec{r}_\alpha \cdot \vec{e}_y) / r_\alpha$, where \vec{r}_α is the vector between the centers of the particles forming the contact α . \mathcal{N} is a symmetric operator of dimension $N_c \times N_c$, which can be written as $\mathcal{N} \equiv \mathcal{T}^t \mathcal{T}$. \mathcal{T} is the operator of dimension $N D \times N_c$ that assigns to any set of N_c contact forces $|f\rangle$ the associated net unbalanced forces $|F\rangle$ appearing on the particles [20]:

$$|F\rangle = \mathcal{T} |f\rangle \Leftrightarrow \forall i, \vec{F}_i = \sum_{\alpha_i} \vec{n}_{\alpha_i} f_{\alpha_i}, \quad (3)$$

where α_i labels the contacts made by particle i and where $\vec{n}_\alpha = \vec{r}_\alpha / r_\alpha$. The non-zero elements of \mathcal{T} thus correspond to the unit vectors \vec{n}_α . \mathcal{T}^t is its transpose.

Previously, we have numerically performed [16] a spectral analysis of $\mathcal{N} \equiv \sum_\omega \omega^2 |f_\omega\rangle \langle f_\omega|$ in flow and found that: (i) the spectrum of \mathcal{N} displays bi-scaling and consists of two structures: one isolated mode of frequency ω_{\min} , and a plateau of modes appearing above a frequency $\omega^* \sim p^{-\delta}$ with $\delta \approx 0.35$, as shown in Fig. 2c,d. (ii) The divergence of the viscosity is governed by the lowest frequency modes $|f_{\min}\rangle$, which has a finite projection on the shear direction

$$\lim_{N \rightarrow \infty} \langle f_{\min} | \gamma \rangle / (||f_{\min}|| \times ||\gamma||) = O(1) > 0. \quad (4)$$

According to Eq.(1) this observation implies that $\eta \sim p \sim 1/\omega_{\min}^2$, as shown in Fig. 3c.

In this Letter we show that these observations, together with the dependence of viscosity on coordination, can be explained by one assumption only, namely that the configurations with coordination z visited by the dynamics are similar to shear-jammed configurations (of friction μ^* and of coordination z_c) where contacts carrying the smallest forces are removed until the coordination is z . The term “similarity” is used here to indicate that the rheological

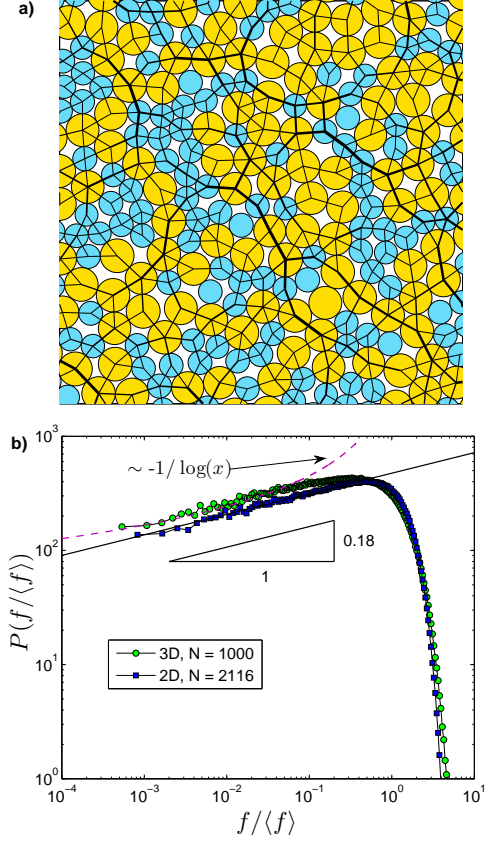


Fig. 1: **a)** Snapshot of a shear-jammed configuration in 2D. The thickness of the lines are proportional to the contact forces, the components of $|\tilde{f}_0\rangle$, see text. **b)** Distributions of the contact forces in shear-jammed configurations; the dashed curve is a fit of the 3D distribution to the functional form $P(x) \sim -1/\log(x)$, and the black line is a power-law with exponent $\theta = 0.18$.

properties of the two models, i.e. the real configurations found in flow and the constructed ones, fall in the same universality class. The rationale for this similarity is that during flow, a negative selection of the weak contacts occurs: indeed only contacts with a small force are fragile, i.e. tend to open and disappear as flow progresses. On the other hand, new contacts are formed by collision and can immediately carry a significant force. Our rule to generate configurations is the simplest one that captures such a negative selection and can be analyzed analytically.

To check our assumption, we use an event-driven code [21] to simulate flow. We simulate systems under simple shear flow with $N = 1000$ particles in three dimensions, using Lees-Edwards periodic boundary conditions [22], at the volume fraction $\phi = 0.644 < \phi_c$. Half of the particles are small and half are large; we set the diameter ratio of small and large particles to be 1.4. At large densities jamming can occur spontaneously when the coordi-

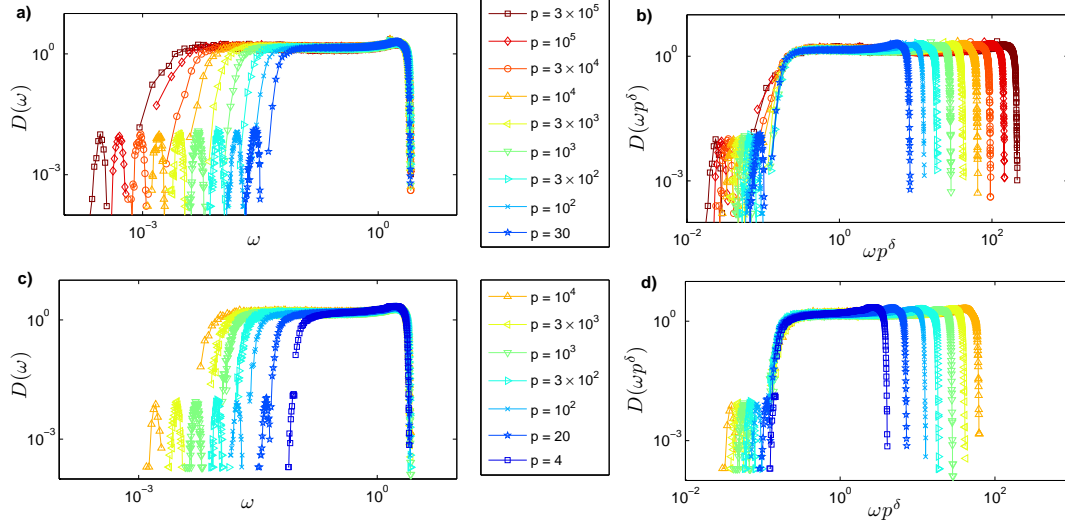


Fig. 2: **a)** Average spectra $D(\omega)$ of the operator \mathcal{N} *v.s.* frequency ω measured for configurations constructed from shear-jammed configurations by gradually removing contacts carrying the weakest forces, see text for details. The spectra are measured by binning the constructed configurations according to their various pressures p as indicated in the legend. The peak at low frequency corresponds to one mode, and has been amplified by some factor for visibility. **b)** $D(\omega)$ *v.s.* rescaled frequency ωp^δ with $\delta = 0.35$. Note the collapse of the onset of the plateau of modes. **c)** $D(\omega)$ *v.s.* frequency ω of the operator \mathcal{N} , measured for the configurations generated in simulations of flow [16]. For each pressure, the spectra are averaged over at least 300 independent flow configurations. **d)** $D(\omega)$ *v.s.* rescaled frequency ωp^δ with $\delta = 0.35$ [16].

nation fluctuates up to $z = z_c$ (see [21] for details), generating anisotropic configurations with an effective friction $\mu = \mu^*$. We consider shear-jammed configurations that jam after a shear strain of at least 200% is imposed on an isotropic system. After averaging over 300 shear-jammed states we obtain an average friction coefficient $\langle \mu^* \rangle = 0.125$, with a standard deviation $\sqrt{\langle (\mu^* - \langle \mu^* \rangle)^2 \rangle} = 0.017$, indicating that finite size fluctuations are small. This result is consistent with previous observations [23] showing that μ^* is a self-averaging quantity, whose standard deviation decreases as $1/\sqrt{N}$.

At jamming $\eta = \infty$ and according to Eq.(1) there must be one normalized mode $|\tilde{f}_0\rangle$ such that $\tilde{\mathcal{N}}|\tilde{f}_0\rangle = 0$. Henceforth we use the tilde notation to refer to quantities characterizing shear-jammed configurations. Thus

$$0 = \langle \tilde{f}_0 | \tilde{\mathcal{N}} | \tilde{f}_0 \rangle = \langle \tilde{f}_0 | \tilde{\mathcal{T}}^t \tilde{\mathcal{T}} | \tilde{f}_0 \rangle = ||\tilde{\mathcal{T}}|\tilde{f}_0\rangle||^2, \quad (5)$$

implying, together with the definition of $\tilde{\mathcal{T}}$, that $|\tilde{f}_0\rangle$ is the vector of contact forces that maintain force-balance. An example of $|\tilde{f}_0\rangle$ is shown in Fig.(1), together with the distribution of the contact forces computed over 300 shear-jammed configurations. The distribution of low forces is of particular importance, and we find that $P(f/\langle f \rangle) \sim (f/\langle f \rangle)^\theta$ with $\theta \approx 0.18$. This scaling relation holds well for two decades for $D = 2$. Such small exponents are hard to distinguish from the case where $\theta = 0$ with logarithmic correction, although the power law fits data better, especially for $D = 2$, see Fig.(1).

We next apply the following procedure to each three-

dimensional shear-jammed state: contact forces are sorted, and the $m \equiv \tilde{N}_c(z_c - z)/z_c$ weakest contacts are removed from the contact network, starting from $m = 1$. Physically, removing a contact corresponds to eroding the particles at the contact point, so that a finite gap appears. Mathematically, one simply does not include these contacts when computing the operator \mathcal{T} defined in Eq.(3). For each m we recompute the associated matrix $\mathcal{N} \equiv \mathcal{T}^t \mathcal{T}$ of dimension $N_c \times N_c$ with $N_c = \tilde{N}_c - m$.

We now argue that these constructed configurations are accurate models of configurations actually visited in flow. We first compare the spectra of \mathcal{N} in the two cases and show that they scale similarly with pressure. Numerical diagonalization of \mathcal{N} readily gives the density of states $D(\omega)$, displayed in Fig.2a for our constructed configurations and in Fig.2c for configurations from flow simulations. These quantities are indeed nearly identical, since both (i) exhibit a plateau of modes above some frequency scale $\omega^* \sim p^{-\delta}$ ($\sim z_c - z$, see below) as proven by the collapse of the plateaus onsets in the right panels of Fig.2, and (ii) display a minimum frequency ω_{\min} , which does not scale with pressure as ω^* does, as shown by the lack of data collapse of the low-frequency peak of $D(\omega)$ in the right panels of Fig.2. We indeed find that $\omega_{\min} \sim 1/\sqrt{p}$ for our constructed configurations shown in Fig.3a, which is also true in flow as recalled in Fig.3c. We note that the width of the low-frequency peak of $D(\omega)$ does not grow with increasing pressure, which indicates that the fluctuations in the spectra of \mathcal{N} are indeed well-controlled. This

is further supported by the limited spread of the clouds of points of Fig.3,a and c, which represent our entire data-set.

Next, we test whether our scheme correctly predicts the divergence of pressure (or viscosity) with coordination observed in flows. Fig.3b shows the pressure p vs. $\delta z \equiv z_c - z$ for each constructed configuration, and Fig.3d represents the same quantity measured in flow. Remarkably, the scaling law $p \sim \delta z^{-1/\delta}$ with $\delta \approx 0.35$ holds for both ensembles of configurations.

We now perform a scaling analysis of the properties of our constructed configurations. We remove a fraction $\delta z/z_c$ of the weakest contacts (i.e. the smallest components of $|\tilde{f}_0\rangle$) and consider the operator \mathcal{N} associated with the constructed configuration. We start by deriving an upper bound for the minimal eigenvalue ω_{\min}^2 of \mathcal{N} , and an lower bound for the viscosity. \mathcal{N} is symmetric hence $\omega_{\min}^2 \leq \langle x|\mathcal{N}|x\rangle$ for any normalized vector $|x\rangle$. We consider the vector $|f_0\rangle$, the projection of $|\tilde{f}_0\rangle$ on the $N_c = (1 - \delta z/z_c)N_c$ remaining contacts. Obviously $\lim_{\delta z \rightarrow 0} \|f_0\| = \|\tilde{f}_0\| \equiv 1$, thus:

$$\omega_{\min}^2 \leq \frac{\langle f_0|\mathcal{N}|f_0\rangle}{\|f_0\|^2} \approx \langle f_0|\mathcal{N}|f_0\rangle \equiv \|\mathcal{T}|f_0\rangle\|^2 = \|F_0\|^2, \quad (6)$$

where $\|F_0\|$ is the norm of the unbalanced force field associated with the contact force $|f_0\rangle$. Removed contacts from a jammed configuration leads to unbalanced forces on particles which lost one or more contacts. In particular, when a contact α with a force f_α is removed, each of the two adjacent particles carries an unbalanced total force of amplitude f_α . In the limit $\delta z \ll 1$ most particles, whose total force is unbalanced, have only lost one contact. Thus:

$$\|F_0\|^2 \approx 2 \sum_{\alpha_r} f_{\alpha_r}^2 = 2N_c \int_0^{f^*} P(f) f^2 df, \quad (7)$$

where the sum is taken over all the removed contacts α_r . Here $P(f)$ is the distribution of the components of the vector $|\tilde{f}_0\rangle$ and f^* is defined as $\int_0^{f^*} P(f) df = \delta z/z_c$. As Fig.1 indicates, we observe that at low forces, $P(f/\langle f \rangle) \sim (f/\langle f \rangle)^\theta$, where the factor $1/\sqrt{N_c} \sim \langle f \rangle$ stems from the normalization of the vector $|\tilde{f}_0\rangle$. We thus obtain two of our main predictions:

$$\begin{aligned} \frac{f^*}{\langle f \rangle} &\sim \delta z^{\frac{1}{1+\theta}}, \\ \omega_{\min}^2 &\leq \delta z^{\frac{3+\theta}{1+\theta}}. \end{aligned} \quad (8)$$

Eq.(8) predicts the emergence of a characteristic force scale in flows, that vanishes in relative terms as jamming is approached. In order to test this prediction we measure in flow the distributions of contact forces for various pressures, see Fig.4a. We observe an erosion in the distribution $P(f/p)$ of relative contact forces f/p , with a characteristic relative force that indeed decays near jamming. To probe

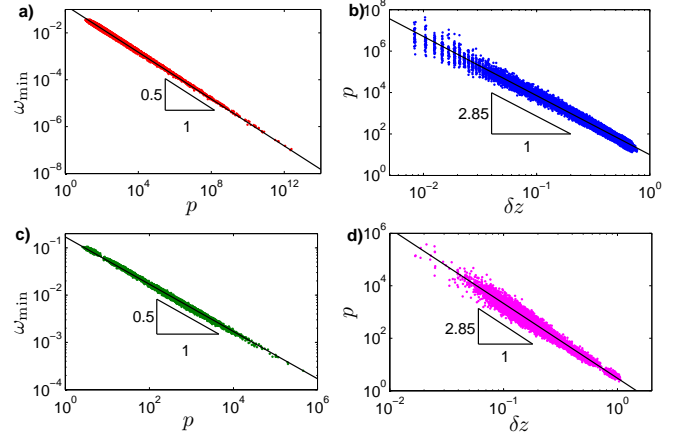


Fig. 3: Minimal frequency ω_{\min} of the operator \mathcal{N} for our constructed configurations **a)** and for configurations from simulations of flow **c)**. Pressure p vs. distance to threshold coordination $\delta z = z_c - z$ for constructed configurations **b)** and for flow **d)**. These data are well-captured by the relations $\omega_{\min} \sim 1/\sqrt{p}$ and $p \sim \delta z^{-1/\delta}$ with $\delta \approx 0.35$ for both ensembles of configurations.

the scaling of this characteristic force, we seek a rescaling of the contact force f/f^* by some f^* that collapses the low-force tail of the distribution. The best collapse is found for $f^* \sim p\delta z \sim p^{1-\delta}$. As indicated in Table 1, this finding corresponds to our prediction for $\theta = 0$, and is still very close to our prediction using $\theta = 0.18$. We note the difficulty in extracting the force scale f^* , as the crossover of the distributions of forces towards the eroded regime is rather weak. Interestingly, we find that the rescaled distributions $P(f/f^*)$ scale as $(f/f^*)^\chi$ with an exponent $\chi \approx 0.38$.

We now test the inequality (9). Assuming that this upper bound is saturated, as expected if the present variational argument captures the essential physics, leads to a prediction for the scaling relation between ω_{\min} and δz . As shown in Table 1, this prediction is in very good agreement with our observations.

As noted above, $D(\omega)$ also displays a frequency scale $\omega^* \sim \delta z \gg \omega_{\min}$ above which a plateau of modes appears. For completeness, we comment on $D(\omega)$ in the frequency range $[\omega_{\min}, \omega^*]$. Although it cannot be observed in our numerics due to the limited size of our systems, normal modes must be present in this interval. Indeed, a local operator like \mathcal{N} cannot have a single lowest eigenvalue ω_{\min}^2 separated from the rest of the spectrum. This can be seen as follows: if $|f_{\min}\rangle$ is the eigenvector corresponding to the eigenvalue ω_{\min}^2 , consider the family of eigenvectors $|f_{\vec{q}}\rangle$ build by modulating $|f_{\min}\rangle$ by plane waves: $f_{\vec{q},\alpha} = \exp(i\vec{q} \cdot \vec{\alpha}) f_{\min,\alpha}$, where $\vec{\alpha}$ is the position of contact α . The set of vectors $|f_{\vec{q}}\rangle$ are approximatively orthonormal $\langle f_{\vec{q}}|f_{\vec{q}}\rangle \approx \delta_{\vec{q},\vec{q}'}$. Furthermore, for small wave vectors

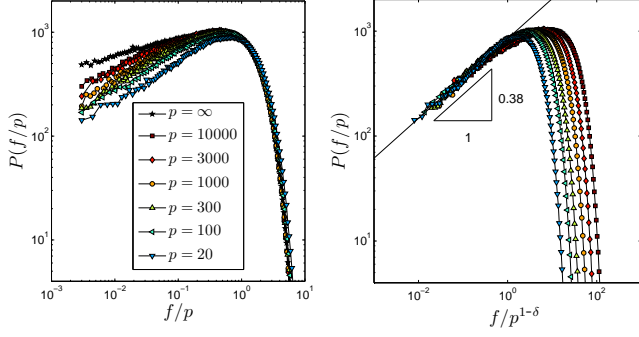


Fig. 4: **a)** Distributions $P(f/p)$ of contact forces f rescaled by the pressure p measured in flow and shear-jammed configurations. Measurements in flow are done at various p , as indicated in the legend. $P(f/p)$ erodes at low f/p as the pressure diminishes away from the jamming threshold. **b)** Distributions of contact forces vs. rescaled force $f/(p\delta z) \sim f/p^{1-\delta}$. This rescaling leads to the collapse of the distribution at small force, indicating the presence of a scaling law.

the force balance that was nearly satisfied in $|f_{\min}\rangle$ is only weakly perturbed, and one finds after a simple calculation that $\omega_q^2 \equiv \langle f_q | \mathcal{N} | f_q \rangle = \omega_{\min}^2 + Bq^2$, where B is a constant of order one. Using that the density of wave-vectors grows as $D(q) \sim q^{D-1}$, the density of states of the frequencies ω_q must then grow as $D(\omega) \propto \omega(\omega^2 - \omega_{\min}^2)^{(D-2)/2}$. Although the ω_q^2 are not exact eigenvalues of \mathcal{N} , we expect our estimate for $D(\omega)$ to be qualitatively correct for $\omega \in [\omega_{\min}, \omega^*]$.

We now derive the divergence of the viscosity η (or equivalently p since $\eta \sim p$) with coordination. Using the convexity of the inverse function and Eq.(8) leads to:

$$\langle f_0 | \mathcal{N}^{-1} | f_0 \rangle \geq \frac{1}{\langle f_0 | \mathcal{N} | f_0 \rangle} \sim \delta z^{-\frac{3+\theta}{1+\theta}} \quad (10)$$

The finite friction coefficient μ^* in shear-jammed configurations implies that contact forces have a finite projection onto shear:

$$\lim_{\delta z \rightarrow 0} \langle \gamma | f_0 \rangle / \|\gamma\| = \langle \gamma | \tilde{f}_0 \rangle / \|\gamma\| \equiv C > 0. \quad (11)$$

Together with Eqs.(1,10), Eq.(11) leads to:

$$\frac{\eta}{\xi_0} = \frac{\langle \gamma | \mathcal{N}^{-1} | \gamma \rangle}{\Omega} \approx \frac{\langle \gamma | f_0 \rangle^2}{\Omega} \langle f_0 | \mathcal{N}^{-1} | f_0 \rangle \geq C^2 \frac{\|\gamma\|^2}{\Omega} \delta z^{-\frac{3+\theta}{1+\theta}} \quad (12)$$

where we have neglected the contribution to the viscosity stemming from the components of $|\gamma\rangle$ orthogonal to $|f_0\rangle$, which we expect to be small. From the definition of $|\gamma\rangle$ it is clear that $\|\gamma\|^2 \sim d^2 N_c$, whereas $\Omega \sim N_c d^D$. Eq.(12) thus yields the following lower bound for the rescaled viscosity $\eta_r \equiv \eta/(d^{D-2}\xi_0)$:

$$\eta_r \geq A \delta z^{-\frac{3+\theta}{1+\theta}} \quad (13)$$

where A is a constant. Using that $p \sim \eta_r$ we can directly compare this prediction with the observations of Fig.(3). Table 1 shows that the observed scaling law is well-captured by the saturation of Eq.(13).

scaling	prediction $\theta = 0.18$	prediction $\theta = 0$	observation
$f^*/p \sim \delta z^{\frac{1}{1+\theta}}$	0.84	1	1
$\omega_{\min}^2 \sim \delta z^{\frac{3+\theta}{1+\theta}}$	2.69	3	2.85
$\eta \sim \delta z^{-\frac{3+\theta}{1+\theta}}$	-2.69	-3	-2.85

Table 1: Predicted scaling exponents and exponents measured numerically in flow. Comparisons are made using the best fitted exponent $\theta = 0.18$ of the force distribution $P(f)$ of jammed states shown in Fig.1, and $\theta = 0$ assuming that the decay in $P(f)$ is logarithmic.

Conclusion. – In flow, the contact network constantly evolves, or rewires, via the formation and opening of contacts. We have shown that a key aspect of this process is the negative selection of contacts that weakly affect flow. Taking this effect into account enables one to derive three scaling relations between four exponents. These relations connect the divergence of the viscosity and spectral properties of dense flows to two microscopic quantities: the coordination z and the exponent θ , which characterizes the density of weak contact forces in jammed configurations. Thus to obtain a complete description of the rheology, future works should compute the value of θ – see [24] for recent results in this direction – and the relation between coordination and packing fraction $z(\phi)$. In packings of soft repulsive particles with $\phi > \phi_c$, the coordination is the minimal one that guarantees mechanical stability [25,26], a condition that determines $z(\phi)$. The concept of stability is not applicable for fluids however, and computing $z(\phi)$ in flow will presumably require a detailed description of the rewiring dynamics.

This work has been supported by the Sloan Fellowship, NSF DMR-1105387, the MRSEC program of the NSF DMR-0820341 and Petroleum Research Fund #52031-DNI9. We thank A. Grosberg, E. Vanden-Eijnden and D. Kraft for comments on the manuscript.

REFERENCES

- [1] EINSTEIN A., *Annalen der Physik*, **17** (1905) 549.
- [2] BATCHELOR G., *Journal of Fluid Mechanics*, **83** (1977) 97.
- [3] POULIQUEN O., *Phys. Rev. Lett.*, **93** (2004) 248001.
- [4] OLSSON P., and TEITEL S., *Phys. Rev. Lett.*, **99** (2007) 178001.
- [5] NORDSTROM K. N., VERNEUIL E., ARRATIA P. E., BASU A., ZHANG Z., YODH A. G., GOLLUB J. P., and DURIAN D. J., *Phys. Rev. Lett.*, **105** (2010) 175701.
- [6] HEUSSINGER C., BERTHIER L., and BARRAT J. L., *Europhys. Lett.*, **90** (2010) 20005.
- [7] BOYER F., GUAZZELLI E., and POULIQUEN O., *Phys. Rev. Lett.*, **107** (2011) 188301.

- [8] LESPIAT R., COHEN-ADDAD S., and HÖHLER R., *Phys. Rev. Lett.*, **106** (2011) 148302.
- [9] LEMAÎTRE A., ROUX J.-N., and CHEVOIR F., *Rheologica Acta*, **48** (2009) 925.
- [10] DA CRUZ F., EMAM S., PROCHNOW M., ROUX J.-N., and CHEVOIR F., *Phys. Rev. E*, **72** (2005) 021309.
- [11] JOP P., POULIQUEN O., and FORTERRE Y., *Nature*, **441** (2006) 727.
- [12] STARON L., LAGREE P.-Y., JOSSERAND C., and LHUILIER D., *Physics of fluids*, **22** (2010) 113303.
- [13] OLSSON P. and TEITEL S., *Phys. Rev. E*, **83** (2011) 030302.
- [14] HEUSSINGER C. and BARRAT J.-L., *Phys. Rev. Lett.*, **102** (2009) 218303.
- [15] HATANO T., *Phys. Rev. E*, **79** (2008) 050301(R).
- [16] LERNER E., DÜRING G., and WYART M., *Proc. Natl. Acad. Sci.*, **109** (2012) 4798.
- [17] We account for finite-size corrections in z_c , see e.g. Goodrich C. P., Liu A. J., and Nagel S. R., *Phys. Rev. Lett.* **109**, (2012) 095704.
- [18] PEYNEAU P.-E. and ROUX J.-N., *Phys. Rev. E*, **78** (2008) 041307.
- [19] N. XU and C. S. O’HERN, *Phys. Rev. E*, **73** (2006) 061303.
- [20] CALLADINE C.R., *Int. J. Solids Struct.*, **14** (1978) 161.
- [21] LERNER E., DÜRING G., and WYART M., *arXiv*., **1111.7225** (2011) .
- [22] ALLEN M. P. and TILDESLEY D. J., *Computer Simulations of Liquids* (Oxford Univ. Press, New York) 1991.
- [23] PEYNEAU P.-E. and ROUX J.-N., *Phys. Rev. E*, **78** (2008) 011307.
- [24] WYART M., *Stability at Random Close Packing*, to be published in *Phys. Rev. Lett.*, also *arXiv:1202.0259* (2012)
- [25] WYART M., SILBERT L. E., NAGEL S. R., and WITTEN T. A., *Phys. Rev. E*, **72** (2005) 051306.
- [26] WYART M., *Annales de Phys*, **30 (3)** (2005) 1.